International Journal of Advanced Research in Physical Science (IJARPS)
Volume 6, Issue 3, 2019, PP 5-23
ISSN No. (Online) 2349-7882
www.arcjournals.org

How the Entanglement Hologram Enhances the Nuclear Fusion and the Battery Effect of Light Irradiation of Hydrogen/ Deuterons Layer on Metals and Graphene

Stefan Mehedinteanu

CITON — Center of Technology and Engineering for Nuclear Projects (retired) Atomistilor no. 409, Bucharest-Magurele, Romania

Corresponding Author:** ***Stefan Mehedinteanu, *CITON — Center of Technology and Engineering for Nuclear Projects (retired) Atomistilor no. 409, Bucharest-Magurele, Romania*

Abstract: *Based on the previously author works about models on nucleons structure and on the bias current inside valence nucleons during β – decay stimulation by a laser, in the present one is analyzed the feasibility of these experiments. Thus, by using QM&MD programme: fhi98md is confirmed the apparition of high Hydrogen (Deuterium) coverage (at ~pm distances) of the surface of Pd lattice, mainly due of the Hydrogen or Deuterium ions screening by Pd valence electrons, the same for the graphene case. Also is proved the author's model of vortex assisted photon beta decay, when a laser photon makes this process much more probable by creating a spot (melt) in nucleon with suppressed order parameter that lowering the energy barrier for vortex crossing together with an heavy electron (bias current $e^{\pm}$) as resulting inside nucleons by a Schwinger effect due of the nucleon's inner Electro-Magnetic (EM) field. Then, if are used lasers of modest power it can appears a net gain of ~20. At this high coverage fraction, the H/D ions at a deep screening near ground state is followed by an electron expulsion, and of proton charge neutralized (like a neutron). Also, it is found that the entanglement of inside nucleons quarks can produce a permanent hologram (spacetime deformation) around nucleons, just when these one were born, respectively, at Universe Confinement Epoch.*

The spacetime deformed ~ 10nm that permits the fall (Casimir effect attraction) of neighborhood nucleons if at this distance penetrates the screening of the ions (H/D) due of metal/graphene electrons, and of ions oneself electrons' production due of LASER irradiation, thus, it is created a battery effect and eventually the enhancement of ions fusion.

Keywords: *nuclear fusion, entanglement, β – decay, alternative energy source, Laser irradiation, instant electrical current, QM&MD programme*

1. THE STATE OF ART

Based on the previously author works about models on nucleons structure and on the bias current inside valence nucleons during $\beta - decay$ stimulation by a laser, in the present one is analyzed the feasibility of some experiments to prove this theoretical finding Mehedinteanu (2015).

The adsorption and absorption of hydrogen on palladium are described in Aldag and Schmidt (1994), when the binding energies of about 22, 25, and 35 kcal/mole were observed, and the saturation coverage at 300 °K was 0.39 H/Pd and at 200 °K this value was increased to 0.95 H/Pd.

In Manchester and San-Martin (1994), the neutron diffraction studies have shown that hydrogen atoms randomly occupy the octahedral interstices in the metal lattice (in a fcc lattice there is one *octahedral* hole per metal atom). The limit of absorption at normal pressures is $PdH_{0.7}$, indicating that approximately 70% of the octahedral holes are occupied. The absorption of hydrogen is reversible, and hydrogen rapidly diffuses through the metal lattice.

The process of surface absorption of hydrogen has been shown by scanning tunneling to require aggregates of at least three vacancies on the surface of the crystal to promote the dissociation of the hydrogen molecule. Mitsui and Fomin (2003).

Since the structure of the atoms is:

Pd: [Kr] $4d^{10}$ 2, 8, 18, 18; Kr: [Ar] $3d^{10}$ $4s^2$ $4p^6$ 2, 8, 18, 8

Ar: [Ne] $3s^2\ 3p^6$ 2, 8 ,8 Ne: [He] $2s^2\ 2p^6$ He: $1s^2$ 2, in order to obtain the inputs fort.11 and fort.12 together with start.inp for fhi98start and fhi98md we use for fhiPP the input:

fort_22.inp for Pd

46.00 8 3 8 0.00 : z nc nv iexc rnlc

1 0 2.00 : n l f

2 0 2.00

2 1 6.00

3 0 2.00

3 1 6.00

3 2 10.00

4 0 2.00

4 1 6.00

4 2 9.00

5 0 1.00

5 1 0.00

2 h : lmax type

Xenon

[Kr] $4d^{10}\ 5s^2\ 5p^6$

per shell 2, 8, 18, 18, 8

^{135}**Xe** syn 9.14 h β^- 1.16MeV ^{135}Cs

Fort_22.inp for Xe

54.00 9 2 8 0.00 : z nc nv iexc rnlc

1 0 2.00 : n l f

2 0 2.00

2 1 6.00

3 0 2.00

3 1 6.00

3 2 10.00

4 0 2.00

4 1 6.00

4 2 10.00

5 0 2.00

5 1 6.00

2 h : lmax s_pp_def

An atom's nth electron shell can accommodate $2n^2$ electrons

Core charge can also be calculated as 'atomic number' minus 'all electrons except those in the outer shell'. For example: Chlorine (element 17), with electron configuration $1s^2\ 2s^2\ 2p^6\ 3s^2\ 3p^5$, has 17 protons and 10 inner shell electrons (2 in the first shell, and 8 in the second) so:

Core charge = 17 − 10 = +7

A subshell is the set of states defined by a common azimuthal quantum number, ℓ, within a shell. The values ℓ = 0, 1, 2, 3 correspond to the *s*, *p*, *d*, and *f* labels, respectively. The maximum number of electrons that can be placed in a subshell is given by 2(2ℓ + 1). This gives two electrons in an s subshell, six electrons in a p subshell, ten electrons in a d subshell and fourteen electrons in an f subshell.

In Lischka and Axel Groß (2003), about the interaction of hydrogen with palladium surfaces, although bulk palladium can absorb large amounts of hydrogen, the most favorable position for hydrogen is on the surface, not in the bulk. Here, the adsorption energy of atomic H on Pd(100) in the fourfold hollow ~ 0.45 eV and in the bridge position ~0.15 eV that are near constant as a function of the coverage (0.25÷1), that were determined by density functional theory calculations within the local density approximation (LDA) using the FP-LMTO method and by DFT calculations employing the generalized gradient approximation (GGA) for the exchange-correlation functional and using ultrasoft pseudotentials (US-PP). The coverage is defined as the number of hydrogen atoms per primitive surface unit cell. Adsorption in the fourfold hollow position is much more favorable than at the bridge position. This is a general trend for hydrogen adsorption on low-index Pd surfaces: hydrogen generally prefers to adsorb at the highly coordinated sites.

In Gruber (2016), they report on the ability of freestanding single layer graphene to provide tens of electrons for charge neutralization of a slow highly charged ion within a few femto seconds. The amount of charge transferred to the highly charged ions (HCI) can be estimated by measuring the distribution of exit charge states q_{out} and the energy of highly charged ${}^{124}_{54}Xe$ ions ($(Z=54; n=70)$ after transmission through single layer graphene (SLG).

Initial ion charge states of $10 < q_{in} < 35$ and velocities below 0.5 nmfs^{-1} were used. Ions are transmitted through SLG under normal incidence and analyzed with respect to their charge state and kinetic energy by an electrostatic analyzer. $h = 3.4\text{Å}$ is the width of the graphene layer. In this case, the elastic collisions (nuclear stopping) may cause direct knockout of carbon atoms, but less than one carbon atom is sputtered on average by a 10–100 keV Xe ions. Even if point defects are produced, they will likely disappear due to dissociation of ubiquitous hydrocarbon molecules. The absence of any traces of large-scale lattice deformations thus confirms the intrinsic ability of suspended SLG to locally sustain exceptionally high current densities, even though it cannot efficiently diffuse heat to a substrate.

The HCI starts capturing electrons from graphene already at 9Å. The strong attractive potential accelerates electrons towards the HCI and, approximately, half of them end up captured by it along the incoming path before penetration into the graphene sheet. The induced electronic charge density as the HCI approaches the graphene layer has two components : one is formed by the convoy electrons around the HCI position, forming an asymmetric wake potential that slows down the ion, and the other one is located at the graphene layer due to the target polarization. Both components merge as the HCI gets closer to the target and forward electron emission starts. Finally, after crossing the layer the projectile is nearly neutralized and the corresponding induced electronic charge is centered around the HCI along its outgoing path. The actual HCI is probably not fully relaxed at the instant of crossing the graphene layer and, therefore, it still suffers a number of autoionization processes and subsequent de-excitation without a significant energy loss.

These results are in range of the experimentally Gruber (2016) determined energy loss for ions with exit charge state $q_{out} = 2$ and $q_{out} = 4$ as a function of the incident charge state q_{in}, around 3.2keV for $q_{in} = 32$. The energy of the projectiles was kept constant for all q_{in} at $E = 40keV$. Here is calculated that HCIs with initial charge states $q_{in} = 10$, 20 and 40 capture ~9, ~17 and ~34 electrons during the passage through the graphene layer, respectively.

Also, Holmid (2017) have obtained a release of mesons (muons) but with a different explanation.

In the following, we can say that these experimental results legitimate more our previously works Mehedinteanu (2007), when we substitute the ruly pseudo-potential (QM-code input) for hydrogenlike atoms (including alpha) with the *screened Coulomb potential* as deduced from the well-known Gamow alpha decay theory.

Potential energy (chemisorptions) of a H atom over a fcc hollow site of a Pd(111) surface as a function of the distance from the surface for a frozen substrate , have been determined by DFT-GGA calculations as of ~-0.23÷0.3÷0.2eV for distances ~-1÷0÷1 Å, for a coverage of θ= 1, and of θ= 1/3.

In present work we done a similar calculation with the program **fhi98md** Bockstedte and Kley (1997), Fuchs and M. Bockstedte (1998).

In the following being calculated the electrical current as resulting from laser irradiation of these H(D) Pd coverage.

2. THE EVALUATION OF PD-D REACTIONS WITH QM&MD PROGRAMME: FHI96MD

This it was demonstrated by using a code package **fhi98md** which is an efficient code to perform density-functional theory (DFT) total-energy calculations for materials ranging insulators to transition metals. The package employs first-principles pseudo-potentials, and a plane-wave basis-set, and is used to done a special calculus for some metals (Pd) where are depozided on the surface and implanted interstitially 1;2;3 H ions.

The package **fhi98md** is an efficient code to perform density-functional theory total-energy calculations for materials ranging insulators to transition metals. The package employs first-principles pseudo potentials, and a plane-wave basis-set. For exchange and correlation both the local density and generalized gradient approximations are implemented.

In Polly-atomic systems as for example molecules, crystals, defects in crystals, surfaces, it is highly desirable to perform accurate electronic structure calculations, without introducing uncontrollable approximations.

The emergency functional the key variable in DFT is the electron density n (**r**).

Consequently, the complementary tool from the all package FHIPP it was used to obtain the pseudo-potentials of H(D), Pd. Thus, is suficiently to substitute the ruly pseudo-potential (QM-code input) for hydrogenlike atoms (including alpha) with the screened Coulomb potential as deduced from the well-known Gamow alpha decay theory.

All that our suggest to use for hydrogen-like atoms (for other atoms are kept the original formulations) the pseudo-potential form, so neglecting the non-local contributions at the level of atom itself, respectively:

$$= \frac{1}{[4\pi\varepsilon_o]} \frac{Z_\alpha Z_D e^2}{r} \qquad for \quad r \geq R$$

In [1] cited in Mehedinteanu (2007), an explanation of the large screening was suggested by the Debye plasma model applied to the quasi-free metallic electrons. In this approach, they combined the Drude model of metals (with a kinetic energy 0.5 kT for the quasi-free valence electrons) with the Debye model of plasma: the Drude-Debye model, in short Debye model. The electron Debye radius around the deuterons in the lattice is given by

$$R_D = \left(\varepsilon_0 kT / e^2 n_{eff} \rho_a\right)^{1/2} = 69(T / n_{eff} \rho_a)^{1/2} \text{ [m]},$$

with the temperature T of the quasi-free electrons in units K, n_{eff} the number of thesis electrons per metallic atom and the atomic density ρ_a in units of atoms m^{-3}. For T = 293 K , $\rho_a = 6 \times 10^{28} m^{-3}$, and $n_{eff} = 1$, is obtained a radius R_D, which is about a factor 10 smaller than the Bohr radius of a hydrogen atom, therefore, we have $r = R_D \cong 0.01 a_0$; $a_0 = 5.29 \times 10^{-11} m$.

The input is obtained with fhi98start applied to files start.inp and inp.mod, that obtaining **inp.ini** as an input to fhi98md plus the pseudo pontetials fort for each species Mehedinteanu (2007). In figure 1(a,b,c,d) are presented the *quart-octahedral* holes in Pd lattice where are placed H(D) atoms. Thus, the main results of application are for: a),b),c) : respectively, simple *quart-octahedral* Pd4 we have : (non-eq) total energy = -78. a.u., for 1 D atom in the proximity of 1Pd (at 0.05Bohrs) of an internal energy at zero temperature = - a.u., see fig. 1(b)

Palladium 1 -2.6175 -2.6175 0.0000

Palladium 2 2.6175 2.6175 0.0000

Palladium 3 2.6175 -2.6175 5.2350

Palladium 4 -2.6175 2.6175 5.2350

Hydrogen 1 0.0000 0.0000 2.6384

The significative difference being: (-233 -(-78))x27.2=-4.18keV, for Pd-4 electrons-valence

Near0.01Bohrs distance between H-H, fig.1c

Atomic positions tau0 :

Species Nr. x y z

Palladium 1 -2.6175 -2.6175 0.0000

Palladium 2 2.6175 2.6175 0.0000

Palladium 3 2.6175 -2.6175 5.2350

Palladium 4 -2.6175 2.6175 5.2350

Hydrogen 1 0.0000 0.0000 2.6175

Hydrogen 2 0.0000 0.0000 2.6280

When, the internal energy at zero temperature = -331 a.u. (Pd- 4 valence electrons)

The difference (-331a.u.- (-78.991727))x27.2=-6.8keV

Pd4H4-fig.1d with the "extracted Hs to be visible"

Palladium 1 0.0000 0.0000 0.0000

Palladium 2 5.2350 5.2350 0.0000

Palladium 3 5.2350 0.0000 5.2350

Palladium 4 0.0000 5.2350 5.2350

Hydrogen 1 2.6175 2.6175 2.6175

Hydrogen 2 2.6175 2.6175 2.6280

Hydrogen 3 2.6489 2.6175 2.6280

Hydrogen 4 2.6175 2.6489 2.6280

internal energy at zero temperature = -630.947097 a.u.

The difference (-630a.u.- (-78.991727))x27.2=-14.9keV

Pd-He-Hf-fig. 1eI and fig. 1eII with alpha particle (He^{+2}) "extracted to be visible

Atomic positions tau0 :

Species Nr. x y z

Palladium 1 -2.6175 -2.6175 0.0000

Palladium 2 2.6175 2.6175 0.0000

Palladium 3 2.6175 -2.6175 5.2350

Palladium 4 -2.6175 2.6175 5.2350

Helium 1 0.0000 0.0000 2.6175

Hafnium 1 0.0000 0.0000 2.6594

internal energy at zero temperature = -4147.420020 a.u.

The difference (-4147 a.u.- (-78.991727))x27.2=-110keV

PdHe=fig. 1eAtomic positions tau0:

Species Nr. x y z

Palladium 1 -2.6175 -2.6175 0.0000

Palladium 2 2.6175 2.6175 0.0000

Palladium 3 2.6175 -2.6175 5.2350

Palladium 4 -2.6175 2.6175 5.2350

Xenon 1 0.0000 0.0000 2.6384

internal energy at zero temperature = -475 a.u.

The difference (-475 a.u.- (-78.991727))x27.2=-10.7 keV

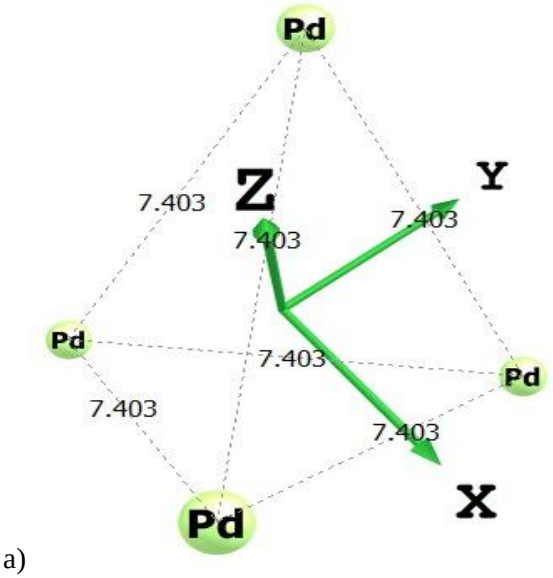

a)

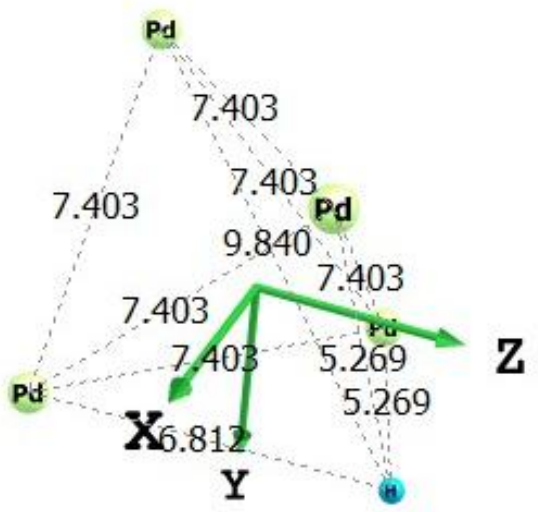

b)

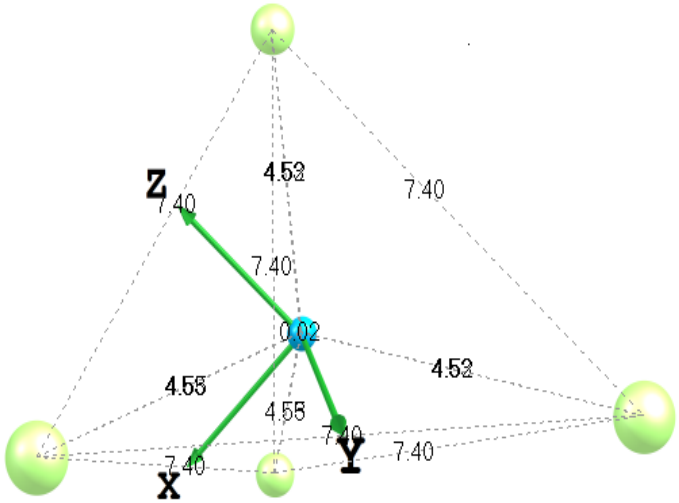

c)

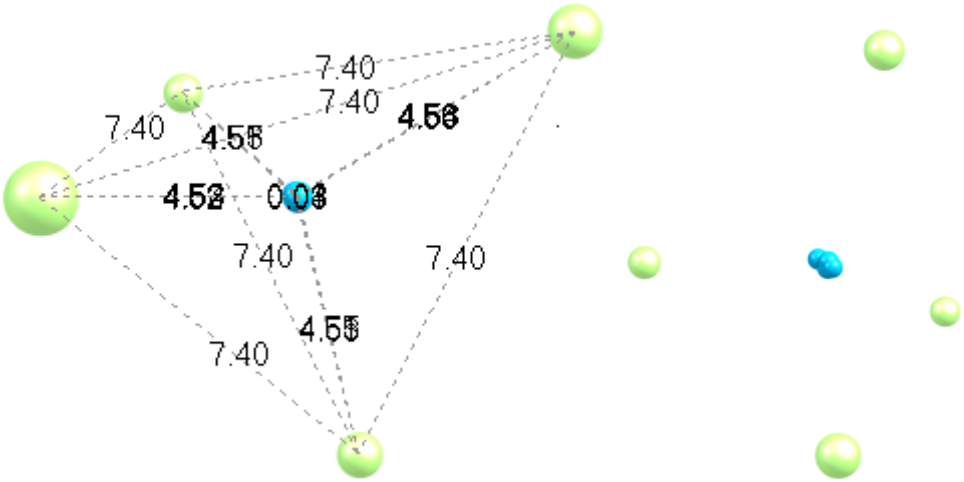

1d)

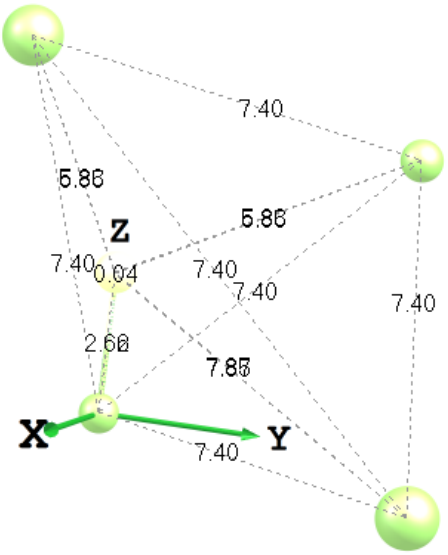

1e-I)

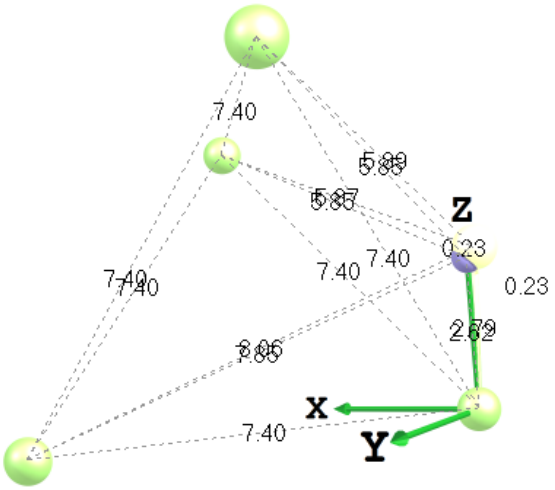

1e-II)

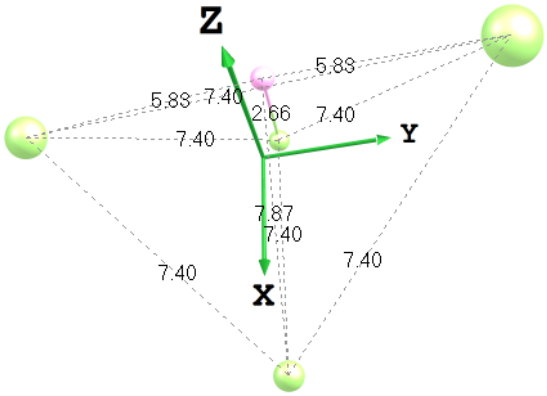

1f)

Fig1. *The quart-octahedral hole of Pd-H coordinates.*

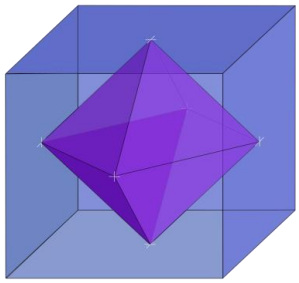

a)

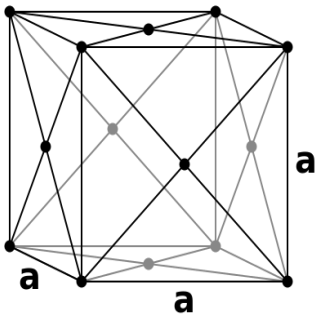

b)

Fig2. *Paladium structure*

3. How can obtain an electrical current (battery) on metallic support of H/D layer or graphene as induced by laser pulses

3.1. The Bias Current Model of β – decay Stimulation by a Thermal Spike of a Photon

In order to accelerate the β – decay by a single photon reaction, a new model it was proposed in Mehedinteanu (2007), Mehedinteanu (2012), Mehedinteanu (2015) to calculate a direct reaction of single photon with one of nucleon of the valence n-n; p-p; n-p pairs (see IBM model refs [30,31] cited in Mehedinteanu (2007) of the nucleus, that being in the unstable state (a *β – decay* nuclide), they are the most susceptible to react with the photon, see some of model's results from Mehedinteanu (2007), figures $1 \div 4$, respectively.

The interaction between a photon of high energy and of low band width $\Delta E/E \le 10^{-3}$ and of nucleon into state of excitation has been characterized by the beta decay energy Q_β from the nuclei, that is viewed as a *direct reaction*, without the formation of a compound nucleus.

Essentially, the general picture of this model described in details in Mehedinteanu (2012a), Mehedinteanu (2015), (Bulaevski et al.2011), (Bulaevski et al, 2012), is that the vortex figure 3.) crossing may trigger the $s \to n$ transition. A photon makes this process much more probable by creating a spot (melt) with suppressed order parameter and thus with lower energy barrier for vortex crossing. A sketch of the strip and of the belt across are shown in Figure 4, the induced vortex crossing together with an electron (*travel current* $e^{\pm}$), which turns superconducting hot belt into the normal state resulting in a vortex assisted photon beta decay.

As a consequence of the Lorentz force acting on a vortex crossing a thin and narrow current-biased strip the energy $\Phi_0 I/c$ is released, which for currents I > 0.6Ic suffices to create a normal belt across the entire width w of the strip (extending to a few correlation lengths ξ along the strip).

Therefore, by using the same nucleon model we can account for a inside nucleon vortex assisted photon count rate, as in Mehedinteanu (2012a), Mehedinteanu (2015), Mehedinteanu (2012b)

$$R_{pc} = R_h\left[1 - \exp(-\Re)\right]$$

,where:

$$R_\nu(I,\nu_h) = \frac{4k_B T R_{eff}}{\pi\Phi_0^2}\frac{\xi}{w}\left(\frac{\nu_h}{2\pi}\right)^{1/2}\left(\frac{I}{I_{ch}}\right)^{\nu_h+1}$$

$$\Re \approx \frac{\tau_{GL}R_\nu}{\nu_0 - \nu_h}\frac{1-(I_{ch}/I)^{\nu_h-\nu_1-1}}{\ln(I_{ch}/I)}$$

The current being

$$I_{ch} = I_{c0}\left(\nu_h/\nu_0\right)^{3/2}$$

$$I_{c0} = \frac{\pi c^2\Phi_0\varepsilon_0}{8\left(2\pi^3 x\lambda^5\right)^{1/2}}e^{-x/\lambda}\times 10^{15}[A/fm^2]$$

The effective ohmic resistance is $R_{eff} = R_s R/(R_s + 2\pi(\xi/w)^2 R)$.

We can suppose than along the hot belt induced by the incident photon, the charge e^- creates a *bias current* $(I > 2/3e[(1/(\nu_h/\nu_0)^{3/2}) \cong 3] \Rightarrow 2e$, see below, who circulates due of the potential difference between the vortex and the rest of isotope.

At the first sight, the ohmic resistance of this ad-hoc electrical circuit created by the *bias current* is given as:

$$R^{-1}=\frac{U_\beta}{\tau_{GL}}\frac{1}{V_{vortex}^2}$$

,where the vortex potential is $V_{vortex}=H_0\xi$,

H_0-an "external" electro-magnetic field of a dipole created by the pair $u\bar{u}$ (the chromoelectrical field)

$$H_0=E_0=\frac{de}{4\pi\varepsilon_0 r^3}=8.33e24\left[\frac{N}{C}\right]$$

,where, $r\cong 0.05[fm]$-is the electrical flux tube radius, $d=0.7[fm]$-the distance between the two quarks charges, usually $H[A/m]$, but here is used as $B=\mu_0 H\left[\frac{J}{Am^2}\right]$

, and the characteristic distance $\xi\le\lambda$, the coherence length, either, we can use the results of section 4., and the power is $U_\beta/\tau\cong\varepsilon_{vortex(W^\pm)}/\tau$, with $\tau_{GL}=\pi\hbar/(8k_BT_c)=1.5e-24[s]$-the Ginzburg-Landau life time of $q^\pm$, where U_β is given by the vortex energy:

$\varepsilon_{vortex}=Vc^2\varepsilon_0H_0^2/8\pi=1.16e-08[J]$,where V-is the volume, see 3, accordingly, the corresponding equivalently masses are $M=\varepsilon_{vortex}/c^2\Rightarrow 73[GeV]$, which seems to be equal to the mass of $W^\pm$ boson generated here by the decay of quarks (Feynman diagram), $V=4\pi\cdot 0.48^3\cdot n_s/3=0.46$, $n_s=1$, the afferent number of gluons.

Numerically, with $T_{c\_11}=5\times10^{11}K$ (ELI laser); and $T_{c\_9}=10^9K$ (Nd:YAG laser), $E_{prag\_11}=k_BT_{c\_11}\cong 43MeV$; $E_{prag\_9}=0.09MeV$ result $\nu_0=\varepsilon_W/k_BT_C=1.e-09/(1.38e-23*2.e12)=36.2$, where $T_c=10^{12}K$ at confinement for one flux tube ($\cong 5.3\times10^{-11}J\rightarrow 330MeV$), and where ε_W results from eq. (27) from Mehedinteanu (2012a) as due of two quarks flux tubes interactions $\varepsilon_W=\varepsilon_{\text{int}}(d=x-\lambda;x=0.14)*0.117[fm]\cong 1.e-09[J]$; $R^{-1}=143\Omega$; $R_s=1000\Omega$; $R_{eff}=141\Omega, w\cong 1fm$.

With $\Phi_0=2\times10^{-15}[Tm^2]$; $\lambda=0.117\,fm$; $x\cong\lambda$, it results $I_{c0}\cong 3.6\times10^7[A/fm^2]$, $I_{c0q}=I_{c0}.q_{rate}=3.6x10^7.10^{-8}=0.36[A/fm^2]$

$\nu_{h\_11}=\varepsilon_{0h}/E_{prag\_11}=5\times10^{-11}/E_{prag\_11}=6.9$,

$\nu_{h\_9}=\varepsilon_{0h\_9}/E_{prag\_9}=9.6\times10^{-14}/E_{prag\_9}=6.9$; that results $R_\nu=3.7\times10^{18}s^{-1}$

The total power per pulse of Nd:YAG laser is $P_{tot}=9.6\times10^{-14}\cdot5\times10^{13}=4.6[J]$

$I_{ch}=I/I_{c0}\cdot3.6\times10^7\times area\times rate\_q^\pm=5\times10^6\cdot10^{-8}=50[mA]$, $area=1fm^2$; the production rate of $q^\pm=R/V\cdot V_{matter}=1.4\times10^{-8}$, see section 4. below, $U=R_{eff}I\cong 7[V]$; $I/I_{c0}=0.138$ as obtained by trials (figure 5), and where ε_{0h} is obtained by using the lower critical field

$$B_0=H_{c1}=\frac{2\Phi_0}{2\pi\lambda^2}\log\left(\frac{\lambda}{\xi}\right)=\frac{\pi\hbar c}{\pi\lambda^2 c}\log(\kappa)=1.e15\left[\frac{J}{Am^2}\right]$$

and with $x\cong\xi=0.107[fm]$;

respectively: $\varepsilon_{0h} = Vc^2\varepsilon_0(2H_{c1})^2/8\pi = 5.3e-11[J] \to 330MeV$, the models of section 4., see below, finally strength these author previously approach based on Ginzburg-Landau Theory.

Similarly values are obtained if we use the consideration given in section 4., when is coupled with the Universe evolution, respectively the confinement epoch-the born of the nucleons.

In our first case of *muons born* due of hot spot $\nu_h = 330MeV / E_{prag} = 7.68$ which is obtained by trials. Thus we obtain the average (dc) voltage $V_{dc} = \Phi_0/c \cdot R_\nu \to 7400V$. We obtain $\tau_0 \approx$ d^2 $\Phi_0/(2\pi\xi^2\ 2cR_{eff}\ I)$, I=50mA, d=1pm, $\tau_0 = 9ns$, the time-of-flight. In fact, this estimate coincides with the time it takes a vortex to cross the strip being pushed solely by the Lorentz force. With these it results $R_\nu=10^{18}$/s.

The value of E_{prag} is determined by trials in order to have $R_{pc}/R_h \cong 1$, see figure 5.

The model results show that in order to have *instant rates(100% decay)*, or a beta decay rate of $R_{pc} = 5\times10^{13} counts/s$, with the incident of single photons rate of $R_{ph} = 5\times10^{13} counts/s$, $R_{pc}/R_h \cong 1$, for all beta-decay isotopes, i.e. these rates are not dependent of the nuclide type, the photons energy needs to be above a threshold energy value of very precise value $5\times10^{11}K \to 43MeV$, but in this case we don't have a net energy gain due of the small current $I_{ch} = 5\times10^{-2}[A]$ due of permanent rate of quarks as the source for further electrons (muons) production by Schwinger effect $R/V \cdot V_{matter} = 1.4\times10^{-8}$ inside the nucleon (see section below), which can decay into heavy-electrons (muons) but more sure into electrons. In the second case of Nd:YAG laser when $T \cong 0.4\times10^9 K$, the power released by the electrical current is $P_W = RI_{ch}^2 = 0.35[w]$ for each deuteron spike, but for an entirely laser wave (10^{13}photons) when pass along a $30\mu m$ (Nd:YAG) it means a total power $P_{tot} = 0.35\times(30\mu m/8Bohrs)^2 \cong 2\times10^9[w]$, for an absorption coverage area of Pd/H~1; 1 Bohr=5.29x10^{-11}[m], or about $\sim 2x10^9/10^8 = 20$ than the power used to produce a such laser spot $\approx 10^8[w]$, as in the following. These values are in case of ELI-laser when: the power is ~2Pw, the flux ~10^{13}ph/s; flux~10^{24}w/m^2, or the extracted power is lower~ 1.4x10^8/2x10^{15}=0.7x10^{-7} times that used by the laser, or without any energy gain. But we can obtain a net energy gain if we use, for example, a smaller laser Nd:YAG when the flux ~10^{13}ph/s, or $T \approx 10^9 K$, but not smaller than this lower limit value, since the current through the "hot belt" is the same i.e. ~ I_{ch}.

A Nd:YAG laser with pulse energy of < 0.2 J is recommended to be used, with 5 ns pulses (or $P_W = 0.1J/5ns = 10^8[w]$) at 532 nm and normally 10 Hz repetition rate , of 0.2 J pulses with 5 ns pulse length ejects ions with energies in the MeV range. The *ns*-resolved signal to a collector can be observed directly on an oscilloscope, showing ions arriving with energies in the range 2-14 MeV/u at flight times 12-100 *ns*, mainly protons from $n \to p$ transformation , and deuterons ejected by proton collisions. An expected signal at *several mA peak current* corresponds to 1×10^{13} particles released per laser shot and to an energy release > 1 J assuming isotropic formation and average particle energy of 3MeV as observed, or $\cong 0.1J/10^{13} \cong 10^{-14} \cong \varepsilon_{0h\_9} = 9.6\times10^{-14}[J] \to 0.6MeV$ which is just the mass of electron, and $\tau \cong \hbar/10^{-14}J \cong 10^{-20}s$, or in term of pulse duration $\tau = 5ns/10^{13} \cong 5\times10^{-22}[s] \rhd \tau_{q^\pm} = 3\times10^{-25}s$, see the next section.

The results from our calculation, in fact the proton it could be due of the transformation a neutron of deuteron into proton ($n \to p + e^-$) by the laser stimulated beta decay, so there is "not any fusion", see below. If an experiment it will be done, that it will be for the first time when the findings confirm author's models, the most important are, the particles energy in MeV range, and the electrical current of ~*few mA*, remaining to be confirmed the number of particles, respectively of ~10^{10} per laser shot.

To note, that if the external binding energy is not lower as in case of free neutrons decay, the barrier is not quickly penetrated by the $e^{\pm}$ assaults, so, these recombine, but, that happens if this barrier is melted by a the LASER spot.

This vortex-assisted mechanism may be verified by application of magnetic fields, which effectively enhance I_{ch} along with the vortex crossing rates but do not affect the creation of hot spots by photons.

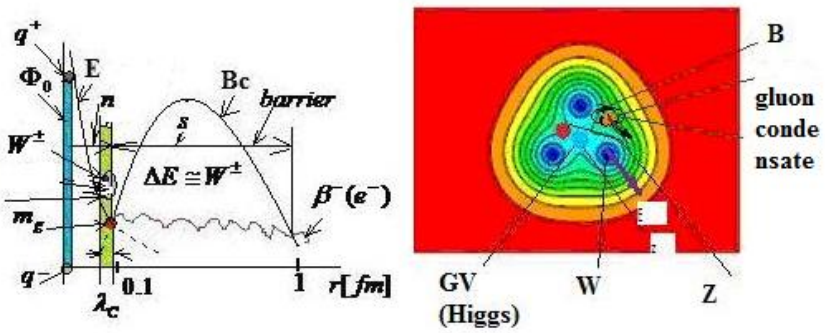

Fig3. *Abrikosov's triangular lattice of flux tubes for a nucleon (author's proposal)*

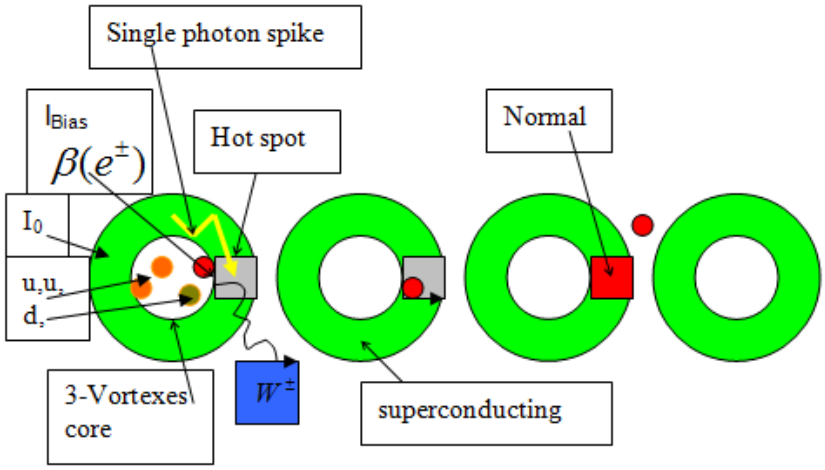

Fig4. *The photonuclear mechanism. From left to right, illustration of incident photon creating superconducting hot spot (hot belt) across nucleon, followed by a thermally induced vortex crossing together with an electron (bias current), which turns superconducting hot belt into the normal state resulting in a vortex assisted photon beta decay.*

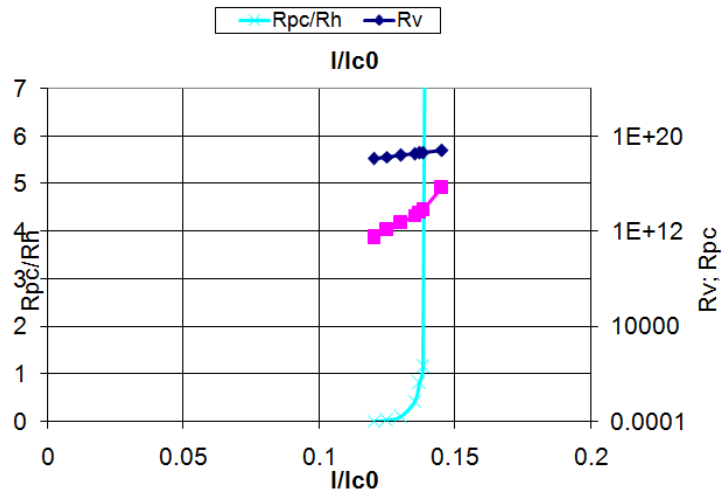

Fig5. *The vortex-assisted photon count rate* R_{pc}/R_h *vs. bias current*

4. MAGNETIC FIELD GENERATION AT THE CONFINEMENT MECHANISM EPOCH

At present, we have no analytic proof of the existence of the condensate of abelian magnetic monopoles in gluodynamics and in chromodynamics.

However, there are two large gaps between QCD and the dual-superconductor picture, as says Dario Grasso.

1. The dual-superconductor picture is based on the Abelian gauge theory subject to the Maxwell type equations, while QCD is a non-Abelian gauge theory.

2. The dual-superconductor picture requires color-magnetic monopole condensation as the key concept, while QCD does not have such a monopole as the elementary degrees of freedom.

Tsuneo Suzuki (2004) founds another confinement mechanism. In this note, where is sown that the dual Meissner effect in an Abelian sense works good even when monopoles do not exist, performing Monte-Carlo simulations of quenched SU(2) QCD with Landau gauge fixing. Instead of monopoles, time-dependent Abelian magnetic fields regarded as magnetic displacement currents are squeezing Abelian electric fields. The dual Meissner effect leads us to the dual London equation and the mass generation of the Abelian electric fields which suggests the existence of a dimension 2 gluon condensate. The present numerical results, hence, suggest the Abelian dual Meissner effect is the real universal mechanism of color confinement which has been sought for many years. Moreover the relation of the Abelian dual Meissner effect with the dimension 2 gluon condensate sheds new light on the importance of the gluon condensate, cited [13, 14, 15, 16, 17].

Hence, the Abelian fields satisfy kinematically the simple Abelian Bianchi identity

$$\vec{\nabla}\times\vec{E}_A^a=\partial_4\vec{B}_A^a \qquad \vec{\nabla}\cdot\vec{B}_A^a=0 \tag{1}$$

The dual Meissner effect says that the squeezing of the electric flux occurs due to cancellation of the Coulombic electric fields and those from solenoidal magnetic currents.

Now what happens in a smooth gauge like the Landau gauge where monopoles do not exist? From Eq.(1), only $\partial_4\vec{B}_A$ regarded as a magnetic displacement current could play the role of the solenoidal current.

It is very interesting to see Fig.4 from Tsuneo Suzuki (2004), in which this happens actually in Landau gauge. Note that the solenoidal current has a direction squeezing the Coulombic electric field. Let us see also the detailed distributions shown in Fig.5 from Tsuneo Suzuki (2004). The other components of the magnetic displacement current $\partial_4 B_{Ar}$ and $\partial_4 B_{Az}$ are not vanishing but they are much suppressed consistently with Fig.2 from Tsuneo Suzuki (2004). In comparison, we show the case of MA gauge also in Fig.5 of Tsuneo Suzuki (2004).

Now they have shown that the magnetic displacement currents are important in the dual Meissner effect when there are no monopoles. Then how can we understand the origin of the dual Meissner effect without monopoles?. The Abelian dual Meissner effect indicates the massiveness of the Abelian electric field as an asymptotic field.

4.1. Dimension 2 Gluon Condensate

Now, Tsuneo Suzuki (2004) shown that the magnetic displacement currents are important in the dual Meissner effect when there are no monopoles. Then how can we understand the origin of the dual Meissner effect without monopoles? The Abelian dual Meissner effect indicates the massiveness of the Abelian electric field as an asymptotic field:

$$(\partial_\rho^2-m^2)\vec{E}_A\approx 0 \tag{2}$$

This leads us to a dual London equation which is a key to the dual Meissner effect. Let us evaluate the curl of the magnetic displacement current. Using Eq.(1), we get

$$\vec{\nabla}\times\partial_4\vec{B}_A=\vec{\nabla}(\nabla\cdot\vec{E}_A)-\vec{\nabla}^2\vec{E}_A$$

From Eq.(2), we get the dual London equation:

$$\vec{\nabla}\times\partial_4\vec{B}_A \approx (\partial_4^2 - m^2)\vec{E}_A \tag{3}$$

Neglecting gauge-fixing and Fadeev-Popov terms, we have equations of motion $D_\mu^{ab}F_\mu^b = 0$ and the (non-Abelian) Bianchi identity $D_\mu^{ab} * F_\mu^{ab} = 0$. Applying D operator to the Bianchi identity and using the Jacobi identity and the equations of motion, we get

$$(D_\rho^2)^{ab}F_\mu^b = 2g\varepsilon^{abc}F_{\mu a}^b F_{va}^c$$

Notice $(D_\rho^2)^{ab} = \partial_\rho^2\delta^{ab} + g\varepsilon^{acb}(\partial_\rho A_\rho^c) + g^2(A_\rho^a A_\rho^b - \delta^{ab}(A_\rho^c)^2)$

Hence if $\langle A_\mu^a A_\nu^b\rangle\delta^{ab}\delta_{\mu\nu}v^2 \neq 0$ we see asymptotically that the electric fields become massive $(\partial_\rho^2 - m^2)E_k^a \approx 0$ with $m^2 = 8g^2v^2$ as of Enrique Ruiz (2004). Now the Abelian electric field is also massive asymptotically $(\partial_\rho^2 - m^2)E_{Ak}^a \approx 0$. Hence, the dual London equation (3) is obtained.

Most estimates in the literature refer to the gluon mass, related to the $m_A^2 = \frac{3}{32}g^2\langle A^2\rangle$ by the formula of Enrique Ruiz (2004),

$$m_A = (625\pm 33)MeV. \tag{4}$$

4.2. Building up Spacetime with Quantum Entanglement

The build of spacetime is obtained by using well-known Inflation models as in A.H.Guth (2004), which in our opinion is nothing else than a spreading of entanglement-energy source-horizon end, where the scale leaving the horizon at a given epoch is directly related to the number $N(\varphi)$ of e-folds of slow-roll inflation that occur after the epoch of horizon exit. Indeed, since H-the Hubble length is slowly varying, we have $d\ln k = d(\ln(aH)) \cong d\ln a = \frac{\dot{a}dt}{a} = Hdt$. From the definition this gives $d\ln k = -dN(\varphi)$, and therefore $\ln(k_{end}/k) = N(\varphi)$, or, $k_{end} = ke^N[m]$, where k_{end} is the scale leaving the horizon at the end of slow-roll inflation, or usually $k^{-1} << k_{end}^{-1}[m]$, the correct equation being $k = k_{end}e^N[m^{-1}]$.

During Universe evolution, the horizon leave is when $a_{leave} = k_{leave}/H_{leave} = 1$, and $k_{leave}^{-1} = H_{leave}^{-1} = 10^{-18}[m]$, .

In the case of a homogeneous potential directed along the z-axis Dario Grasso (2001) eq. (2.2), the Einstein stress-energy tensor is:

$$T^{00} = T^{11} = T^{22} = -T^{33} = \rho = \frac{\varepsilon_0 c^2 B^2}{8\pi};\quad T^{0i} = 0,\quad \text{where } \rho_B[J/m^3]\text{-the magnetic energy density.}$$

$$\varepsilon = \frac{V_{vol}\varepsilon_0 c^2 B^2}{8\pi} = \rho V_{vol} = m_A = V[J], \tag{4'}$$

$V_{vol} = 2\pi\lambda_C\lambda_c(4\lambda_C) \cong 8\pi\lambda_C^3$, at Compton length equally with the penetration length $\lambda_C = \lambda$, that results

$$E^2 = \frac{(V)}{\varepsilon_0(\lambda_C^{e*})^3}$$

With $V = \varepsilon_{gluons}$ as above is obtained $B = E_{q\bar{q}}/c$.

$$\varepsilon = \frac{V_{vol}\varepsilon_0 c^2 B^2}{8\pi} = \rho_B V_{vol} = V = m_A = [J],$$

$V_{vol} = 2\pi\lambda_C\lambda_c(4\lambda_C) \cong 8\pi\lambda_C^3$, at Compton length $\lambda_C = \hbar/mc$

$$E^2 = \frac{(V)}{\varepsilon_0(\lambda_C^{e*})^3} \quad , \text{ also } E = Bc = \frac{\hbar c}{e\lambda_C^2}$$

4.3. Entanglement Hologram around Nucleons at Confinement Epoch

From Mehedinteanu S. (IJARPS-issue 1, 2019) we have for Ryu-Takayanagi (RT) modified formula:

$$\frac{2\pi}{\hbar}\int d^2x\sqrt{g}T_\mu^\mu = \frac{2\pi}{\hbar}\rho_{bulk} = \frac{3H^2}{2\cdot 2\cdot G}n\frac{1}{\hbar}$$

$$\frac{2\pi\cdot c^3\cdot\rho}{\hbar} = \frac{3H^2\cdot c^3}{4G}\frac{1}{\hbar} \quad \text{or} \quad \frac{c^3\cdot\rho}{3\hbar} = \frac{H^2\cdot c^3}{8\pi G}\frac{1}{\hbar} \quad \text{or,} \quad \frac{c^3\cdot\rho\cdot l_P^2}{3\hbar} = H^2[s^{-2}] \text{ , or,}$$

$$\frac{c^3\cdot\rho\cdot l_P^2}{3\hbar}\frac{1}{c^2} = H^2[m^{-2}] \qquad (5)$$

$$\rho\big|_{bulk} = n_{bit\_threads}\rho_{bubble} = n\rho = n\frac{T_j}{c^2\lambda_C^3}$$

For example, $\rho = \dfrac{M_U}{n_{bit\_threads}\cdot\lambda_C^3}$; (5')

$n = n_{bit\_threads} = \dfrac{M_U c^2}{m_A}$; from section 4. below, we appreciate for nucleon $m_A = 1GeV$; $l_P = 7.8\times10^{-35}$

4.4. Deformation of Spacetime around Nucleons

From L.H. Ford (2001) we have:

$\lambda = \kappa^{-1}e^{kv}$; $\kappa^{-1} = 4M$; $v = t + r^*$; $C = 1 - 2M/r$; and $r^* = \int C^{-1}dr$; $C_{,r} = 2M/r^2$

We will assume that $T_{vv}(v)$ represents ingoing/outgoing radiation which changes the black hole's mass by only a small fractional amount, $|\Delta M| << M$. We can then take κ to be constant to lowest order. If we change the independent variable from λ to v = t + r*, then

$$\frac{d}{d\lambda} = e^{-\kappa v}\frac{d}{dv}; \quad v = 1/\omega; \quad \kappa = \frac{c^3}{4GM}$$

And

$$T_{\mu\nu}k^\mu k^\nu = e^{-2\kappa v}T_{vv}$$

For spherically symmetric pulses, the shear and vorticity vanish, and the Raychaudhuri equation, Eq. (36) from L.H. Ford (2001), becomes

$$\frac{d\theta}{dv} = -\frac{1}{2}e^{\kappa v}\theta^2 - 8\pi e^{-\kappa v}T_{vv}(v)$$

The equation for the horizon area can be expressed as

$$\frac{dA}{dv} = e^{\kappa v} A\theta$$

If we take $A_0 = 16M_0^2$ to be the initial area of the black hole in the distant past, where M_0 is its initial mass, then we have

$$\frac{\Delta A}{A_0} \cong \frac{a}{\kappa} e^{\kappa v_+} = 2\frac{\Delta M}{M_0} \tag{6}$$

In this approximation, the change in the mass of the black hole is

$$\Delta M = \frac{a}{2\kappa} M_0 e^{\kappa v_+} = \frac{aA_0}{8\pi} e^{\kappa v}$$

where we have used $\kappa = 1/(4M) \cong 1/(4M_0)$.

This agrees with the result obtained by calculating the change in mass directly from Eq. (4') as

$$\dot{M} = \frac{dM}{dt} = F = \int T_t^r r^2 d\Omega$$

On the horizon, $T_t^r = T_{vv}$, $r = 2M + \varepsilon$

Since the quarks generated inside nucleons are generated by a pulsating process with frequency $v = \omega^{-1}$, a such pulse of stress-energy it could be $8\pi T_{\mu\nu} k^\mu k^\nu = a\delta(\lambda)$, a is a positive constant, and the surface gravity $\kappa = \frac{c^3}{GM}[s^{-1}]$.

We can observe that $\frac{\Delta A}{A} = \frac{8\pi GM}{c^2} \cdot \frac{1}{R} = \frac{r_{Schw}}{R}$, or, we have obtained the classical formula for deformation.

4.5. The Born of Quarks inside the Nucleons as a Permanent Process

Now, the rate per unit volume of quarks pair creation is given by using the Schwinger effect R inside the nucleon, *when this electric field* E *is induced by* $e^+ - e^-$ *quarks pairs which decay in* $q^\pm$ *that explaining* β^- *decay,* of leading order behavior

$$R = (E/E_{cr})^2 (c/\lambda^4)(8\pi^3)^{-1} * \exp(-\pi E_{cr}/E) \tag{7}$$

or $E/E_{cr} << 1$, positron charge e, mass m, Compton wave-length $\lambda_C = \hbar/mc$ and so-called "critical" electric field

$$E_{cr} = m^2 c^3 / e\hbar$$

the volume is given by:

$V_{matter} = (\lambda_C)^4 \frac{1}{c}[m^3 s]$; $m = 330MeV$ the mass of quarks tubes.

The $q^\pm$ rate is $R/V \cdot V_{matter} = 1.4 \times 10^{-8}$, all the time.

4.6. The Entanglement Hologram around Nucleons

From Mehedinteanu S. (IJARPS-issue 10) at the Confinement epoch at hologram site around the nucleon $\varepsilon_{0h}=1/a_{end}=5.24\times10^{-11}J\cong330MeV$ as above; and from inflationary models as above, we have $a_{end}=3$; $k_{end}^{-1}=2.3\times10^{4}[m]$, and with eq. (5) results $R=4.8\times10^{7}[m]$, and $t_{end}=R/c=0.16s$, $\lambda_C=5.7\times10^{-16}[m]$; $H_{leave}^{-1}=k_{leave}^{-1}=10^{-18}[m]$; we found by trials $N=58$. Here in eq. (5) we use $M_U=m_{nucleon}=1.5\times10^{-27}kg$; and results $n_{bit\_threads}=0.26$; $m_A=5.2\times10^{-11}[J]\rightarrow330MeV$, and from eq. (5') the density on hologram is $\rho=2.8\times10^{19}[kg/m^3]$

For spacetime deformation calculation we use the same model of section (4) above as in Mehedinteanu S. (IJARPS-issue 11) , with $a=\frac{c}{R}[s^{-1}]$; where above $R=4.8\times10^{7}[m]$; the surface gravity $\kappa=\frac{c^3}{GM_U}[s^{-1}]$, $.\kappa=4\times10^{62}[s^{-1}]$; $a=6$; with $M=1.5\times10^{-27}[kg]$; if we have the generation with eq. (7) with $E_{cr}=1.71\times10^{23}[N/C]$, and $E=1.7\times10^{23}[N/C]$; $B=E/c=5.6\times10^{14}[T]$ based on $\varepsilon_{0h}\cong\varepsilon_{QCD}\cong5.2\times10^{-11}[J]$ in eq. (5') as mentioned.

And, as in MehedinteanuS. (IJARPS-issue 11) and above it results $\nu=\omega^{-1}=(R/V\cdot V_{vol})^{-1}$; where $R/V\times V_{vol}\cong3.7\times10^{61}\cdot\lambda_C^3=7.4\times10^{15}[s^{-1}]$, $\nu=1.4\times10^{-16}[s]$; and we approximate $e^{\kappa\nu}\cong1+\kappa\nu+...=\kappa\nu=3.6\times10^{46}$; So, the deformation is $\frac{\Delta A}{A}=8\times10^{-16}$ an important initially distortion.

In other words the pulse is entangled at the nucleon outside hologram with $A=R=5\times10^{7}[m]$, that resulting the deformation of the spacetime of $\Delta A=A\cdot8\times10^{-16}=4\times10^{-8}[m]$. With this deformation, and if the electrons screening is realized till there, after that the nucleon enters under the attraction of the neighborhood nucleons like in the Casimir Effect, the LASER melts the coulombic Barrier, that can enhances the nuclear fusion and the release of electrons from inside the nucleon. To note, that this deformation makes possible the nucleons binding into nucleus.

5. CONCLUSIONS

In the work by using QM&MD programmes: **fhi96md** is confirmed a high coverage H/Pd~1 mainly due of a metal-graphene electrons deep screening, that permits a high events density of H/D ions interaction during a laser irradiation followed by a new electrons release.

Thus, there are used the prior author models of vortex assisted photon beta decay, when a laser photon makes this process much more probable by creating a spot (melt) in nucleon with suppressed order parameter that lowering the energy barrier for vortex crossing together with an heavy electron (*bias current* $e^{\pm}$) as resulting from the decay of the of quarks pairs rate $q^{\pm}\cong10^{-8}$ as produced inside nucleons by a Schwinger effect. The electrical power results as P_w=2x10^9 w<<P_{laser}=2Pw for a laser spot of size $30\mu m$, that corresponds with ELI laser characteristics, or without a any net gain of energy.

For the prior author's models validation it is necessarily to do laboratory experiments in the spirit of this work, namely based on the use of a Nd:YAG laser with pulse energy of < 0.2 J, with 5 ns pulses (or $P_W=0.1J/5ns=10^8[w]$) at 532 nm and normally 10 Hz repetition rate. Thus in this case of much smaller power lasers when per photons is obtained ~10^{-5}w x1ns (T=10^{9}K)~10^{-14} J of duration ~*1ns* and, respectively ~10^{-14} J.10^{13} ~0.1J~10^8 [w] for a pulse composed of ~10^{13} ph/s. The net energy

is much higher of $2x10^9/10^8=20$. In such experiments is expected to obtain a particles energy in MeV range, a current of ~*few mA*, a voltage on the shunt 7[V], and the time-of-flight 10^{-8} s.

If these electrons are collected either in the metallic plate in serried into an electrical circuit –a battery arrangement, or into a spherical conductive cover, we can constitute a reliable source of direct electricity with the period equally that of laser pulse frequency. It is possible that the neutron of D do not transforms into proton, since the *open hot belt* created due of the laser photon incidence to *close* after electron passage, therefore it is not a consume of D. To obtain a D LAYER the author calculated that is necessary a thermal energy of 2-3eV to be deposited on the Pd plate in the vacuum chamber containing the D gas, this being in serried into an electrical circuit. If is used the co-deposition Pd/D technique, are obtained also some of cold fusions together with an electrical current, that due of electrons deep screening of deuterons in lattice, as explained by the author early, the same for graphene support.

Since, in hot nuclear fusion (Sun) this process takes place naturally, this electrons excess improves the further screening, that can stabilizes the plasma.

It seem that the extracted energy is from quantum vacuum, or, it could be unfinished, we hope that this work will *fuel* laboratory works.

REFERENCES

S. Mehedinteanu (2015), A new model for w,z, higgs bosons masses calculation and validation tests based on the dual ginzburg-landau theory(revised-2015), http://www.researchgate.net/ profile/Stefan_Mehedinteanu/publications

A.W. Aldag, L.D Schmidt (1994), Interaction of hydrogen with palladium, Journal of Catalysis, Volume 22, Issue 2, August 1971, Pages 260–265; b) *Manchester, F. D.; San-Martin, A.; Pitre, J. M. (1994). "The H-Pd (hydrogen-palladium) System". Journal of Phase Equilibria* ***15****: 62. doi:10.1007/BF02667685*

Fuchs (1998), M. Bockstedte, E.Pehlke, and Scheffer (1998), Physical Rev. B, 57, No.4 (1998) 2134-2145

M. Bockstedte (1997), A. Kley, J. Neugebauer and M. Scheffler (1997): "Density-functional theory calculations for polyatomic systems: Electronic structure, static and elastic properties and Abinitio molecular dynamics", Comp. Phys. Commun. 107, 187 (1997).

L.N. Bulaevskii (2011), M.J. Graf, C.D. Batista, V.G. Kogan (2011), Phys. Rev. B 83,144526 (2011).

L. N. Bulaevskii (2012), Matthias J. Graf, V. G. Kogan (2012), Vortex-assisted photon counts and their magnetic field dependence in single-photon superconducting detectors, arXiv:1108.4004v3 [cond-mat. supr-con], 2012

Elisabeth Gruber (2016) et al. Ultrafast electronic response of graphene to a strong and localized electric field, *Nature Communications* (2016). DOI: 10.1038/ncomms13948

Leif Holmlid (2017): Mesons from Laser-Induced Processes in Ultra-Dense Hydrogen H(0) http://journals.plos.org/plosone/article?id=10.1371/journal.pone.0169895

Markus Lischka and Axel Groß (2003), Hydrogen on palladium, A model system for the interaction of atoms and molecules with metal surfaces, Recent Developments in Vacuum Science and Technology, 2003: 111-132;

S. Mehedinteanu (2007) On The Numerical Analysis Of Decay Rate Enhancement In Metallic Environment, Acta Physica Polonica B No 10, Vol. 38 (2007).

Stefan Mehedinteanu (2012a), On the Photonuclear Rates Calculation for Nuclear Transmutation of Beta Decay Nuclides by Application of the Ginzburg-Landau Theory, Journal of Nuclear and Particle Physics 2012, 2(3): 57-70 DOI: 0.5923/j.jnpp.20120203.05, http://article.sapub.org/10.5923.j.jnpp.20120203.05.html..

Stefan Mehedinteanu (2012b), On the Acceleration of Beta Nuclides Decay by the Photonuclear Reaction, International Journal of Nuclear Energy Science and Engineering (IJNESE) Volume 2, Issue 2 2012 PP. 45-56 www.ijnese.org © World Academic Publishing,

http://www.ijnese.org/paperInfo.aspx?ID=4865

Stefan Mehedinteanu (2015), The Numerical Analysis of Beta Decay Stimulation by the High Thermal Spike of Photon Incidence to Valence nucleons, 2015, http://www.researchgate.net/profile/ Stefan_Mehedinteanu/publications

T. Mitsui (2003), M. K. Rose, E. Fomin, D. F. Ogletree, M. Salmeron (2003), Dissociative hydrogen adsorption on palladium requires aggregates of three or more vacancies, Nature, Volume 422, Issue 6933, pp. 705-707 (2003).

H. Suganuma (2011), T. Iritani, A. Yamamoto, F. Okiharu, T.T. Takahashi (2011), Lattice QCD Study for Confinement in Hadrons, arxiv:1103.4015v1[hep-lat], 2011.

Dario Grasso (2001), Hector R. Rubinstein, Potentials in the Early Universe, arxiv:astro-ph/0009061v2, 2001

Stefan Mehedinteanu (Issue 1), **On the Nature of CMBR Universe Epoch Hologram, International Journal of Advanced Research in Physical Science (IJARPS)** ***Volume 6, Issue 1, 2019, PP 19-30 ISSN No. (Online) 2349-7882 www.arcjournals.org***

Tsuneo Suzuki (2004), Katsuya Ishiguro, Yoshihiro Mori, Toru Sekido, The dual Meissner effect in SU(2) Landau gauge, arxiv:hep-lat/0410039v1, 2004.

Enrique Ruiz Arriola (2004), Patrick Oswald Bowman, Wojciech Broniowsk, Landau-gauge condensates from the quark propagator on the lattice, arxiv:hep-ph/0408309v3, 2004.

a) A. H. Guth (1993), S. Y. Pi, Phys. Rev. Lett. 49 (1982) 1110; b) ALAN H. GUTH, Inflation, arxiv:astro-ph/0404546v1 27Apr 2004; c) Andrew R. Liddle, David H. Lyth, The Cold Dark Matter Density Perturbation arXiv:astr-ph/930.3019v1,1993.

L.H. Ford (2001), Thomas A. Roman, CLASSICAL SCALAR FIELDS AND THE GENERALIZED SECOND LAW, arXiv:gr-qc/0009076v2, 2001.

Stefan Mehedinteanu (Issue 10), **The Lensing Effect a Proof of Large Scale Entanglement in Holographic** CFTs, International Journal of Advanced Research in Physical Science (IJARPS) *Volume 5, Issue 10, 2018, PP 13-23 ISSN No. (Online) 2349-7882 www.arcjournals.org.*

Stefan Mehedinteanu (Issue 11), The Entanglement in Holographic CFTs- an Alternative Explanation of the Binary Black Hole Merger (LIGO) Experiment, International Journal of Advanced Research in Physical Science (IJARPS) Volume 5, Issue 11, 2018, PP 31-42 ISSN No. (Online) 2349-7882 www. arcjournals. org.

Citation: *Stefan Mehedinteanu. "How the Entanglement Hologram Enhances the Nuclear Fusion and the Battery Effect of Light Irradiation of Hydrogen/ Deuterons Layer on Metals and Graphene", International Journal of Advanced Research in Physical Science (IJARPS), vol. 6, no. 3, pp. 5-23, 2019.*

Copyright: *© 2019 Authors, This is an open-access article distributed under the terms of the Creative Commons Attribution License, which permits unrestricted use, distribution, and reproduction in any medium, provided the original author and source are credited.*